

A two-dimensional disordered magnetic metamaterial

Mario I. Molina

Departamento de Física, Facultad de Ciencias, Universidad de Chile, Casilla 653, Santiago, Chile

(Dated: July 17, 2022)

We examine the effect of resonant frequency disorder on the eigenstates and the transport of magnetic energy of a two-dimensional (square) array of split-ring resonators (SRRs). In particular, we focus on two kinds of binary disorder: an uncorrelated one (Anderson) and a correlated one, where tetramers units are assigned at random to lattice sites. This is a direct extension of the random dimer model (RDM) in one-dimensional systems. We find that the absence of any resonant mechanism for transmission of two-dimensional plane waves (which do exist in the one-dimensional case) prevents the SRR array from exhibiting a net transport of magnetic energy. The mapping of the system to a tight-binding model shows that for SRR arrays, there exists a complete correlation between energy disorder and coupling disorder, with a site energy and coupling that are the ‘inverse’ of the usual tight-binding model. The computed shape of the density of states suggests that our SRR system is akin to an effective off-diagonal Anderson system.

Introduction. The recent ability to tailor material properties at will has led to a whole class of artificial materials, termed metamaterials, characterized by unprecedented thermal, optical, and transport properties that make them attractive candidates for current and future technologies. Among them, we have magnetic metamaterials (MMs) that consist on an array of metallic split-ring resonators (SRRs) coupled inductively[1–3]. This type of system can, for instance, feature negative magnetic response in some frequency window, making them attractive for use as a constituent in negative refraction index materials[4–7]. The usual theoretical treatment of such structures is an effective medium approximation where the composite is treated as a homogeneous and isotropic medium, characterized by effective macroscopic parameters. Of course, this approach is valid, as long as the wavelength of the electromagnetic field is much larger than the linear dimensions of the MM constituents.

One of the simplest two-dimensional MM model consists of a periodic square array of split-ring resonators (SRRs) lying on a common plane, where each resonator consists of a small, conducting ring with a slit (Fig1). Each SRR unit in the array is equivalent to a resistor-inductor-capacitor (RLC) circuit featuring self-inductance L , ohmic resistance R , and capacitance C built across the slit. If we assume a negligible resistance, each unit will possess a resonant frequency $\omega = 1/\sqrt{LC}$. Under this condition and in the absence of driving, the evolution equations for the charge Q_n residing at the n th ring are given by

$$\frac{dQ_{\mathbf{n}}}{dt} = I_{\mathbf{n}} \quad (1)$$

$$L \frac{dI_{\mathbf{n}}}{dt} + \frac{Q_{\mathbf{n}}}{C} = -M \sum_{\mathbf{m}} \frac{dI_{\mathbf{m}}}{dt} \quad (2)$$

where M is the mutual inductance and the sum is restricted to nearest-neighbors of \mathbf{n} . These equations can be cast in dimensionless form as

$$\frac{d^2}{dt^2} \left(q_{\mathbf{n}} + \lambda \sum_{\mathbf{m}} q_{\mathbf{m}} \right) + \omega_{\mathbf{n}}^2 q_{\mathbf{n}} = 0 \quad (3)$$

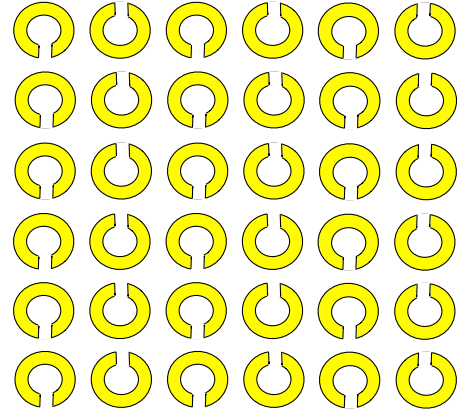


Figure 1. Two-dimensional split-ring resonator array.

where $q_{\mathbf{n}}$ denotes the dimensionless charge of the n th ring, λ is the coupling between neighboring rings that originates from the dipole-dipole interaction, and $\omega_{\mathbf{n}}^2$ is the resonant frequency of the n th ring, normalized to a characteristic frequency of the system, such as the average frequency: $\langle w^2 \rangle = (1/N) \sum_{\mathbf{n}} w_{\mathbf{n}}^2$. We assume that the magnetic component of any incident electromagnetic wave is perpendicular to the SRRs’ plane, and that the electric field of the incoming wave is transverse to the slits. Under these conditions, only the magnetic component of the incoming wave creates an electromotive force on the rings, giving rise to an oscillating current in each SRR and to an oscillating voltage difference across the slits. Also, it is a good idea to minimize electric dipole-dipole effects coming from the strong electric fields at the slits by a judicious placing of the SRRs in the common plane so that the slit-to-slit distance is kept as large as possible (Fig.1). The main drawback of the SRR array is the existence of large ohmic and radiative losses. A possible way to deal with this problem that has been considered is to endow the SRRs with external gain, such as tunnel (Esaki) diodes[8, 9] to compensate for such losses.

The dimensionless stationary state equation is ob-

tained from Eq.(3) after posing $q_{\mathbf{n}}(t) = q_{\mathbf{n}} \exp[i(\Omega t + \phi)]$:

$$-\Omega^2 \left(q_{\mathbf{n}} + \lambda \sum_{\mathbf{m}} q_{\mathbf{m}} \right) + \omega_{\mathbf{n}}^2 q_{\mathbf{n}} = 0. \quad (4)$$

The frequency $\omega_{\mathbf{n}}^2$ can be changed by varying the capacitance of the ring, which is accomplished by altering the slit width or by inserting a dielectric in the slit. For a homogeneous array, $\omega_{\mathbf{n}}^2 = 1$.

On the other hand, the topic of the effect of disorder on the stationary and transport properties of a discrete, periodic system, is an old one, but its importance has not waned throughout the years given its fundamental importance in several fields. The most important result in this area is Anderson localization which asserts that the presence of disorder tends to inhibit the propagation of excitations. In fact, for 1D systems, all the eigenstates are localized and transport is completely inhibited[10–12]. This was also proven to be true in two-dimensional systems, while in three-dimensions a mobility edge is formed. Now, Anderson localization is based on the assumption that the disorder is “perfect” or uncorrelated. However, it has been noted that in one-dimensional lattices with correlated disorder, a degree of transport is still possible. This is the case of the random dimer model (RDM) for the usual tight-binding model. It consists of a binary alloy for the site energies where each site energy is assigned at random to pairs of lattice sites. This leads to a mean square displacement of an initially localized excitation that grows asymptotically as $t^{3/2}$ at low disorder levels, instead of the saturation behavior predicted by Anderson theory[13–15].

An experimental demonstration of the RDM prediction has been made in an optical setting[16]. A straightforward extension of these ideas to random arrays of larger units (n-mers), has also been theoretically explored[17]. In the context of a disordered, one-dimensional SRR array, it was found that an uncorrelated disorder always leads to localization of magnetic energy at any disorder strength, with a transmissivity that decreases exponentially with the size of the system. For correlated disorder and small and medium disorder level, however, it becomes possible for a fraction of states to have resonant transmission, leading to a power-law decrease of the overall transmissivity, with system size[18].

In this work, we examine the localization of the magnetic modes and the transport of magnetic excitations in a two-dimensional disordered square array of split-ring resonators, where the resonant frequencies $\omega_{\mathbf{n}}^2$ in Eq.(4) are taken as random quantities. We will use two different types of randomness: A completely uncorrelated one (i.e., Anderson-like) and a correlated one consisting on a straightforward 2D generalization of the well-known random dimer model used in one-dimensional systems. As expected, in the uncorrelated case we obtain fully localized modes and absence of transport. For the correlated case, we find that unlike the 1D random dimer model, the absence of transmission resonances also leads

to an absence of magnetic transport. These studies give us some inkling as to the magnetic energy transport in higher dimensions, as well as to checking the universality of Anderson localization.

A usual indicator of localization is given by the participation ratio (PR), that measures the extent of the electric charge distribution stored in the capacitors (or magnetic energy density stored in the inductors):

$$PR = \left(\sum_{\mathbf{n}} |q_{\mathbf{n}}(t)|^2 \right)^2 / \sum_{\mathbf{n}} |q_{\mathbf{n}}(t)|^4 \quad (5)$$

For a completely localized excitation, $PR = 1$, while for a complete delocalized state, $PR = N$.

To monitor the degree of mobility of a magnetic excitation we resort to the mean square displacement (MSD) of the charge distribution, defined as

$$\langle \mathbf{n}^2 \rangle = \sum_{\mathbf{n}} \mathbf{n}^2 |q_{\mathbf{n}}(t)|^2 / \sum_{\mathbf{n}} |q_{\mathbf{n}}(t)|^2. \quad (6)$$

Typically $\langle \mathbf{n}^2 \rangle \sim t^\alpha$ at large t , where α is known as the transport exponent. The types of motion are classified according to the value of α : ‘localized’ ($\alpha = 0$), ‘sub-diffusive’ ($0 < \alpha < 1$), ‘diffusive’ ($\alpha = 1$), ‘super-diffusive’ ($1 < \alpha < 2$) and ‘ballistic’ ($\alpha = 2$).

Homogeneous case. Before embarking into the effects of disorder on the system, let us begin by examining the phenomenology in the absence of disorder, $\omega_{\mathbf{n}}^2 = 1$, in order to have a proper comparison context.

After posing $q_{\mathbf{n}} \sim \exp(i\mathbf{k} \cdot \mathbf{n})$ and solving for Ω^2 , we obtain the dispersion relation in d -dimensions as

$$\Omega_{\mathbf{k}}^2 = \frac{1}{1 + \lambda \sum_{\mathbf{m}} \exp(i\mathbf{k} \cdot \mathbf{m})} \quad (7)$$

where the sum is restricted to nearest neighbors.

The time evolution of a completely localized initial charge $q_{\mathbf{n}}(0) = A \delta_{\mathbf{n},0}$, and no currents, $(dq_{\mathbf{n}}/dt)(0) = 0$, is given by

$$q_{\mathbf{n}}(t) = (A/v) \int_{FBZ} e^{i(\mathbf{k} \cdot \mathbf{n} - \Omega_{\mathbf{k}} t)} d\mathbf{k} + (A/v) \int_{FBZ} e^{i(\mathbf{k} \cdot \mathbf{n} + \Omega_{\mathbf{k}} t)} d\mathbf{k} \quad (8)$$

where v is the volume of the first Brillouin zone (FBZ), and $\Omega_{\mathbf{k}}^2$ is given by Eq.(7). After replacing this form for $q_{\mathbf{n}}(t)$ into Eq.(6), one obtains after some algebra, a closed form expression for $\langle \mathbf{n}^2 \rangle$:

$$\langle \mathbf{n}^2 \rangle = \frac{(1/v) \int_{FBZ} (\nabla_{\mathbf{k}} \Omega_{\mathbf{k}})^2 (1 - \cos(2 \Omega_{\mathbf{k}} t))}{1 + (1/v) \int_{FBZ} \cos(2 \Omega_{\mathbf{k}} t)} t^2. \quad (9)$$

At long times $\langle \mathbf{n}^2 \rangle$ approaches a ballistic behavior

$$\langle \mathbf{n}^2 \rangle = \left[\frac{1}{v} \int_{FBZ} (\nabla_{\mathbf{k}} \Omega_{\mathbf{k}})^2 d\mathbf{k} \right] t^2 \quad (t \rightarrow \infty) \quad (10)$$

while at short times,

$$\langle \mathbf{n}^2 \rangle = \left[\frac{1}{v} \int_{FBZ} \Omega_{\mathbf{k}}^2 (\nabla_{\mathbf{k}} \Omega_{\mathbf{k}})^2 d\mathbf{k} \right] t^4 \quad (t \rightarrow 0). \quad (11)$$

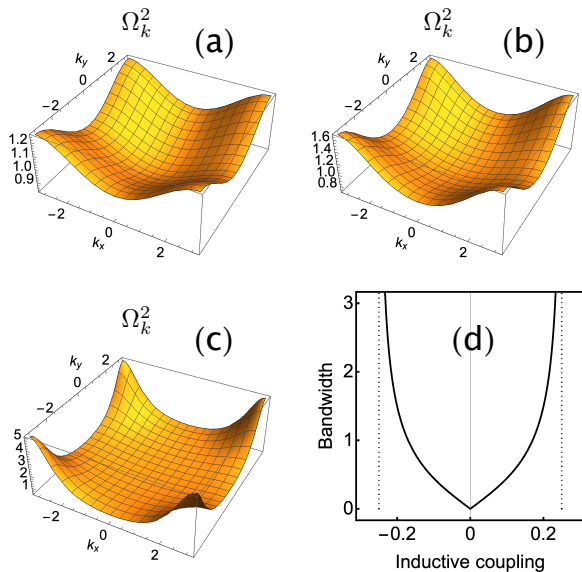


Figure 2. Dispersion relation for homogeneous case: (a) $\lambda = 0.05$ (b) $\lambda = 0.1$, (c) $\lambda = 0.2$ (d) Bandwidth as a function of inductive coupling.

For a square lattice ($d = 2$),

$$\Omega_{\mathbf{k}}^2 = \frac{1}{1 + 2\lambda(\cos(k_x) + \cos(k_y))} \quad (12)$$

where, $\mathbf{k} = (k_x, k_y)$. We see that the system is capable of supporting magnetoinductive waves, if $|\lambda| < 1/4$. The bandwidth, defined as $|\Omega_0^2 - \Omega_{\pm\pi}^2|$ depends directly on λ . Figure 2 shows the band $\Omega_{\mathbf{k}}^2$, as well as the bandwidth. We see that at the edges of the Brillouin zone, the bandwidth diverges at $|\lambda| = 1/4$, but the increase in bandwidth is mostly concentrated in the immediate vicinity of $(k_x, k_y) = (\pm\pi, \pm\pi)$.

Disorder. We introduce now disorder into our system by considering the case when the resonant frequencies $\omega_{\mathbf{n}}^2$ are taken as random. This can be done in practice by altering the spacing between the slits, or by inserting different dielectrics in the slits. Let us get back to the stationary equation (4) which can be rewritten as

$$-\left(\frac{1}{\Omega^2}\right)q_{\mathbf{n}} + \left(\frac{1}{\omega_{\mathbf{n}}^2}\right)q_{\mathbf{n}} + \lambda\left(\frac{1}{\omega_{\mathbf{n}}^2}\right)\sum_{\mathbf{m}}q_{\mathbf{m}} = 0 \quad (13)$$

We see right away that the equation looks similar to an Anderson tight-binding model, with a site energy term equal to $1/\omega_{\mathbf{n}}^2$, and a site-dependent coupling $\lambda/\omega_{\mathbf{n}}^2$. Thus, the ‘‘diagonal’’ term and the ‘‘coupling’’ term are completely correlated, and their values appear ‘‘inverted’’ when compared to a usual tight-binding model.

We will explore two kinds of disorder: an uncorrelated one, where the site frequencies $\omega_{\mathbf{n}}^2$ are assigned at random from a binary distribution $\{1, \omega^2\}$ for a given impurity fraction. Clearly, for $\omega^2 = 1$, we recover the homogeneous

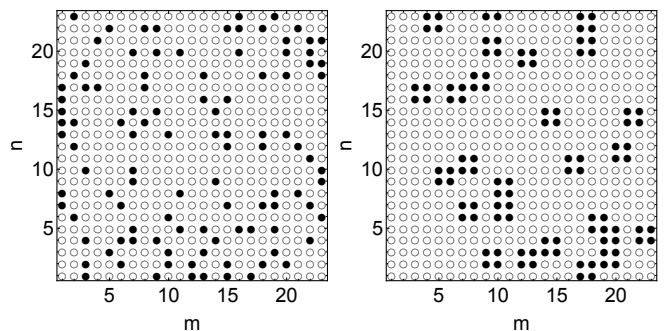


Figure 3. Random realization of an uncorrelated (left) and a correlated (right) distribution of random resonant frequencies. (Impurity fraction: 20%).

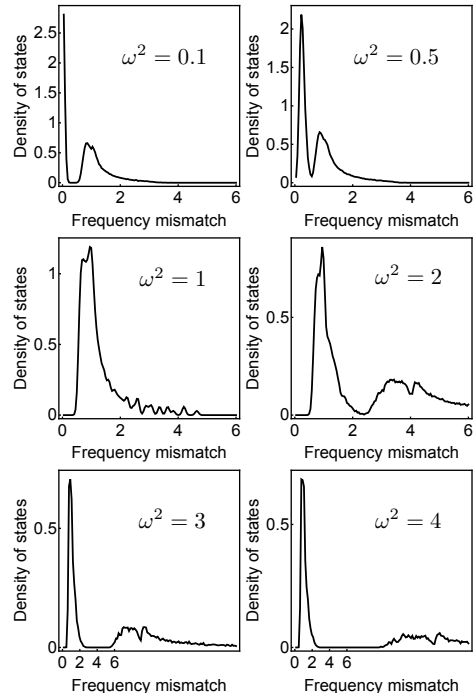


Figure 4. Average density of states for the uncorrelated disorder, for several impurity mismatch values ω^2 ($N = 15 \times 15$, impurity fraction=0.5, number of realizations=33)

case. The second kind of disorder we will explore is a correlated one, inspired by the RDM. While in the RDM one assigns random site frequencies at pairs (dimers) of lattice sites, in our case we assign (random) site energies to 4 nearby sites or ‘‘tetramers’’ of lattice sites. Figure 3 shows an example of a disorder realization for the uncorrelated and correlated cases. We notice the presence of 4-sites clusters that constitute the new ‘‘point impurities’’. Is like having fewer, but larger impurities.

Figure 4 shows the average density of states (DOS)

$$D(\Omega^2) = \left\langle \left(1/N^2\right) \sum_{\mathbf{m}} \delta(\Omega^2 - \Omega_{\mathbf{m}}^2) \right\rangle \quad (14)$$

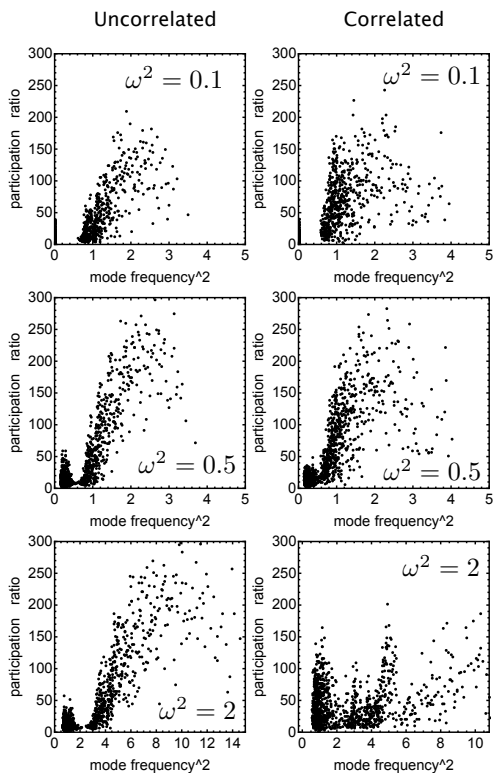


Figure 5. Comparison of the average participation ratio for the uncorrelated (left column) and the correlated case (right column), for the same single random realization and for several impurity mismatch values ω^2 ($N = 33 \times 33$, impurity fraction=0.5.)

where the sum is over all modes. The figure shows the uncorrelated only, since its correlated counterpart is similar (not shown). The no-disorder case ($\omega^2 = 1$) for our finite system seems to hint at the existence of van Hove-like singularities. Given the small size of our lattice is not possible to say more. Also, it seems that some quasi-singularities remain in place at low frequencies and are not removed by the strength of the frequency mismatch. This behavior is reminiscent of the 2D tight-binding Anderson model with off-diagonal disorder, where the singularity is not washed away by the disorder[19]. In our case we have both types of disorder and this would ordinarily mean that the singularity would disappear, however, we have identical values for the site energy and coupling strength for both types of disorder (Eq.(13)). This might explain why our singularities persist even at high mismatch strength. Also, the DOS shows the formation of a quasi-gap at high mismatch strengths that separates a low-frequency sector from a high-frequency lobe that decreases in amplitude as the mismatch strength is increased.

In the absence of disorder ($\omega^2 = 1$) and for a square

lattice of $N \times N$ sites, the participation ratio is[20]

$$\begin{aligned} PR &= \left(\sum_{m_1, m_2} |q_{m_1, m_2}|^2 \right)^2 / \sum_{m_1, m_2} |q_{m_1, m_2}|^4 \\ &= \left(\left(\sum_m |q_m|^2 \right)^2 / \sum_m |q_m|^4 \right)^2, \end{aligned} \quad (15)$$

i.e., the square of the one-dimensional participation ratio for the 1D lattice. Using $q_n \sim \sin(kn)$, we obtain $PR \approx (4/9)N \times N$ in the limit of a large number of sites[20]. Figure 5 shows the participation ratio PR of the eigenstates for a single random realization, for the uncorrelated and correlated cases. In both cases we have employed the same basal binary realization $\{0, 1\}$ and just change the amplitudes. In other words, $\omega_n^2 = \omega^2 \times \{0, 1\}$. The PR in both cases look similar, especially in the low- and medium mismatch disorder strengths. The small value of the PR at low frequencies indicates that localization is stronger there.

Disordered transport. Let us now compute the spreading of an initially localized magnetic excitation and observe its time evolution. A useful quantity to monitor the spreading of an excitation is the mean square displacement (MSD), defined in Eq.(6). We will compute and compare the MSD for the uncorrelated and correlated cases. Results are shown in Fig. 6, where the MSD is computed for several different mismatch values ω^2 . The special case of no disorder $\omega^2 = 1$ is represented by the red curve, and is given in exact form in Eq.(9). As we can see, the behavior for both kinds of disorder is quite similar. In both cases, as ω^2 is increased, the curves become higher and higher and seem to converge towards a eventual plateau. Since, because of computational constraints, we could not set up a large 2D lattice, it is

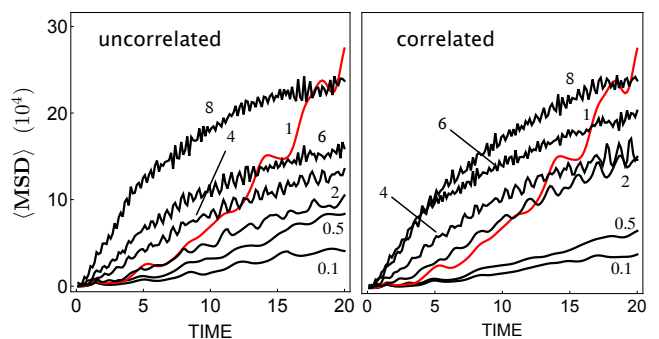


Figure 6. Comparison of the average RMS for the uncorrelated (left column) and the correlated case (right column), for several impurity mismatch values ω^2 ($N = 33 \times 33$, impurity fraction=0.5, number realizations=33.)

not possible to discuss the asymptotic MSD exponent $\langle MSD \rangle \sim t^\alpha$. Something interesting however, that can be observed in Fig. 6, is that except for the case of no disorder, the MSD curves with smaller mismatch ($\omega^2 \ll 1$) converge to saturation faster. This could be due to the observation that, according to Eq.(13), a small value of ω_n^2 gives rise to a higher site ‘disorder’, while at large ω_n^2 we are in the low disorder regime and thus, a slower approach to saturation.

In the one-dimensional case, there is a nontrivial difference between the uncorrelated and correlated case: The existence of resonant trajectories where a plane wave can propagate across the whole lattice without scattering. This happens for energies close enough to the resonant energy where a wave goes through a dimer with unit transmission. This gives rise to \sqrt{N} of transmitting states[13–15]. In two dimensions however, we do not have the possibility of a plane wave resonant transmission across our basic unit (tetramer) and so, we are back to the regular Anderson model for the square lattice. This means transport of magnetic energy is not possible for our system.

Conclusions. We have compared the effect of two types of disorder on the eigenmodes and the transport of excitations, of a simplified model of a magnetic metamaterial consisting of a two-dimensional (square) array of split-

ring resonators. The disorder consisted on random values of the resonant frequencies of the rings, taken from a binary distribution, that are assigned to array sites completely at random (uncorrelated case), or by assigning ‘tetramers’ at random to the array sites (correlated case). The last case corresponds to a generalization of the random ‘dimer’ model for one-dimensional systems. Our system can be mapped to a tight binding system with site energies and couplings that are identical and with effective disorder strength values that are ‘inverted’, Eq.(13). If one of the values of the binary frequencies is taken as unity (a background value), then the strength of the disorder depends on the value of the other frequency: If it is small, the effective disorder of the original system is large, and if it is large, we are in the small disorder regime of the original system. A look at the density of states reveals that for both, the uncorrelated and correlated cases, the system is closer to an off-diagonal Anderson system. The participation ratio and the mean square displacement are similar for both kinds of disorder. This similarity is probably due to the lack of a resonant transmission mechanism (like in the one-dimensional case), rendering the system as a simply disordered one. These results could be of use for the design of efficient magnetic energy confinement devices, and the harvesting and transport of magnetic energy.

-
- [1] N. Katsarakis, G. Constantinidis, A. Kostopoulos, R. S. Penciu, T. F. Gundogdu, M. Kafesaki, E. N. Economou, Th. Koschny and C. M. Soukoulis, *Opt. Lett.* **30**, 1348 (2005).
- [2] M. I. Molina, N. Lazarides, and G. P. Tsironis, *Phys. Rev. E* **80**, 046605 (2009).
- [3] T. J. Yen, W. J. Padilla, N. Fang, D. C. Vier, D. R. Smith, J. B. Pendry, D. N. Basov, and X. Zhang, *Science* **303**, 1494 (2004).
- [4] D. Smith, W. Padilla, D. Vier, S. Nemat-Nasser, and S. Schultz, *Phys. Rev. Lett.* **84**, 4184 (2000).
- [5] V. G. Veselago, *Sov. Phys. Usp.* **10**, 509 (1968).
- [6] J. B. Pendry, A. J. Holden, D. J. Robbins, and W. J. Stewart, *IEEE Trans. Microwave Theory Tech.* **47**, 2075 (1999).
- [7] R. A. Shelby, D. R. Smith, S. Schultz, *Science* **292**, 77 (2001).
- [8] L. Esaki, *Phys. Rev.* **109**, 603 (1958).
- [9] T. Jiang, K. Chang, L.-M. Si, L. Ran, and H. Xin, *Phys. Rev. Lett.* **107**, 205503 (2011).
- [10] P. W. Anderson, *Phys. Rev.* **109**, 1492 (1958).
- [11] B. Kramer and A. MacKinnon, *Rep. Prog. Phys.* **56**, 1496 (1993).
- [12] Elihu Abrahams, *50 Years of Anderson Localization* (World Scientific Publishing, 2010).
- [13] J. C. Flores, *J. Phys. Cond. Matt.* **1**, 8471 (1989).
- [14] D.H Dunlap, H. L. Wu, and P. W. Phillips, *Phys. Rev. Lett.* **65**, 88 (1990).
- [15] D. Giri, P.K. Datta, and K. Kundu, *Phys. Rev. B* **48**, 14113 (1993).
- [16] U. Naether, S. Stuetzer, R. Vicencio, M. I. Molina, A. Tünnermann, S. Nolte, T. Kottos, D. N Christodoulides and A. Szameit, *New J. Phys.* **15**, 013045 (2013).
- [17] D. Lopez and M. I. Molina, *Phys. Rev. E.* **93**, 032205 (2016).
- [18] Mario I. Molina, [arXiv:2008.09550](https://arxiv.org/abs/2008.09550)[cond-mat.dis-nn].
- [19] Wei Min Hu, John D. Dow, and Charles W. Myles, *Phys. Rev. B* **30**, 1720 (1984).
- [20] M. I. Molina, *Phys. Lett. A* **384**, 126704 (2020).

ACKNOWLEDGMENTS

This work was supported by Fondecyt Grant 1200120.